Materials Science in Semiconductor Processing 127 (2021) 105685

Contents lists available at ScienceDirect

Materials Science in Semiconductor Processing

journal homepage: http://www.elsevier.com/locate/mssp

Deep-level transient spectroscopy of GaN grown by electrochemical deposition and irradiated with alpha particles

Abdulraoof I.A. Ali [a,b,*], Helga T. Danga [a], Jacqueline M. Nel [a], Walter E. Meyer [a]

[a] Physics Department, University of Pretoria, Pretoria, 0002, South Africa
[b] Faculty of Education, University of Elimam Elmahdi, Kosti White Nile, Sudan

ARTICLE INFO

Keywords:
Electrochemical deposition
GaN
DLTS
Defects
Irradiation

ABSTRACT

Gallium nitride, which is used in modern electronic devices, is generally grown employing expensive epitaxial techniques. This study investigated the growth of GaN using electrochemical deposition and compared the use of two substrates, silicon (111) and indium tin oxide, under different conditions. Using different characterization techniques, it was found that the properties of the film depended on both the substrate and deposition conditions. X-ray diffraction demonstrated the presence of mainly hexagonal but also a small amount of cubic structures with crystallite sizes ranging from between 11 nm and 18 nm. Schottky diodes were fabricated on the thin films deposited on Si (111) and were characterized using *I-V*, *C-V* and DLTS measurements. The Schottky diodes had a rectification ratio of about 20, a *I-V* barrier height of 0.58 eV, a *C-V* barrier height of 1.18 eV and carrier density of 1.1×10^{18} cm^{-3}. In the as-grown material, only one defect state at 0.32 eV below the conduction band was observed. However, after irradiation with high-energy alpha particles, four defect states at 0.10 eV, 0.20 eV, 0.42 eV and 0.51 eV were observed.

1. Introduction

Group III-nitride semiconductor materials such as GaN, AlN, and InN are promising materials since their properties are ideal for use in opto-electronic devices (e.g. blue/green diode lasers and LEDs) and high power, high-temperature electronic devices [1,2]. These materials have wide band gaps ranging from 1.9 to 6.3 eV. There are many techniques for growing GaN layers, including metal-organic chemical vapor deposition [1], molecular beam epitaxy [3], hydride vapor-phase epitaxy [4] (HVPE) and recently, room-temperature electrochemical growth [5,6]. The advantages of electrochemical deposition are that the growth rate and surface morphology may be controlled by varying the deposition parameters, cost-effectiveness, minimum waste generation, long bath lifetime and easy set-up. GaN can crystallize according to the wurtzite (hexagonal), zinc blende (cubic), and rock salt structures (cubic). The hexagonal structure is the thermodynamically stable structure, while the cubic structures are metastable [7]. As-grown GaN is usually n-type and the carrier concentration is in the order of 10^{18} cm^{-3}. All semiconductors contain defects. They may be impurity atoms or crystalline defects [8]. Some of the defect-introducing mechanisms include material growth, device processing, high-energy particle irradiation [9] and implantation [10]. These defects influence the properties of III-nitride materials in several ways, including reducing the carrier mobility [11]. These defects also influence the *I-V* and *C-V* characteristics of Schottky diodes and maybe further studied through deep-level transient spectroscopy (DLTS).

DLTS is a powerful technique where transients in the capacitance of a diode due to thermal emission of carriers from defects are observed. Thermal scanning is used to detect a wide variety of electron or hole traps in the band gap of the semiconductor [12]. In this study, the room-temperature electrochemical deposition was used to synthesize GaN on n-Si (111) and ITO, and the structural and electrical properties of the material were determined.

Irradiation of the samples allows for the comparison of the defects observed in the electrodeposition-grown material to those in epitaxially-grown material. In addition, GaN is known as a radiation hard material, and it would be interesting to investigate the radiation hardness of the material grown by electrodeposition.

1.1. Experimental

The GaN thin films were prepared on Si (111) and ITO-coated glass

* Corresponding author. Physics Department, University of Pretoria, Pretoria, 0002, South Africa.
E-mail addresses: abdalraof34@gmail.com, aia.ali@up.ac.za (A.I.A. Ali).

https://doi.org/10.1016/j.mssp.2021.105685
Received 24 August 2020; Received in revised form 14 December 2020; Accepted 7 January 2021
Available online 23 January 2021

Table 1
Conditions under which the GaN thin films were deposited.

Sample	Substrate	Current density (mA cm^{-2})	Deposition time (hrs)	Stirring
A	ITO	1	3	Yes
B	ITO	1	12	Yes
C	ITO	0.7	3	No
D	Si	1	0.5	Yes
e	ITO	1	0.5	Yes

Fig. 1. A schematic diagram of the gold Schottky and aluminium Ohmic contacts on n-GaN.

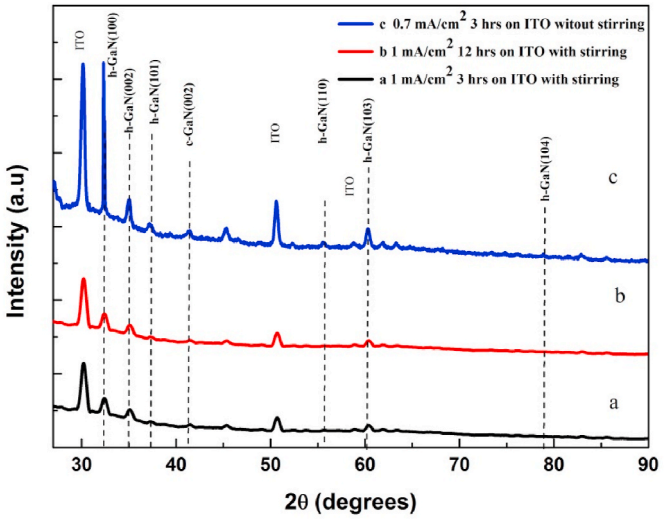

Fig. 2. XRD spectrum for *Samples a*, *b* and *c* deposited at different current densities for different times. The indicated peak positions correspond to h-GaN JCPDS 50–0792.

Table 2
Structural parameters extracted from XRD patterns of the electrochemically deposited GaN thin films on ITO substrates. The full width at half maximum and position of the (100) peak, the crystallite size (*t*), and lattice constants (*a* and *c*) are shown. The (100) peak was used to determine *a* while the (002) peak was used to determine *c*.

Crystal data	FWHM (100) (°)	2θ (100) (°)	*t* at (100) (nm)	Lattice constants (Å)	
				a (100)	*c* (002)
JCPDS-50-7992	–	32.411	–	3.186	5.178
a	0.748	32.407	11	3.183	5.140
b	0.704	32.406	12	3.183	5.142
c	0.501	32.369	18	3.198	5.156

substrates by electrochemical deposition from a solution of 0.02 M Ga $(NO_3)_3$ and 0.01 M NH_4NO_3 in deionized water at room temperature. The technique used a simple electrochemical cell consisting of an anode, a cathode, and an electrolyte. The anode was activated carbon and the cathode was the substrate, either Si or ITO. The GaN thin films were grown using different electrodeposition current densities starting with 1 mA/cm^2 for 3 h on ITO (*Sample a*), 1 mA/cm^2 for 12 h on ITO (*Sample b*), 0.7 mA/cm^2 for 3 h on ITO (*Sample c*), 1 mA/cm^2 for 30 min on Si (*Sample d*) and 1 mA/cm^2 for 30 min on ITO (*Sample e*) as summarised in Table 1. In all cases, except for *Sample c*, the solution was stirred. The thin films were characterized using X-ray diffraction (XRD) and scanning electron microscopy (SEM). Thereafter, Schottky diodes were fabricated on the GaN thin films deposited on Si. Ohmic contacts of 70 nm thick aluminium and Schottky contacts of 0.6 mm diameter and 80 nm thick gold (see Fig. 1) were deposited using a resistive evaporation system. The electrical characterization was done using *I-V, C-V* and DLTS measurements. The effect of radiation damage due to high-energy alpha particles from an americium 241 metal foil with an energy of 5.4 MeV and a fluence rate of 7.1×10^6 cm^{-2} s^{-1} to a fluence of 6.1×10^{11} cm^{-2} on the electrical properties was also investigated.

When gallium nitrate and ammonium nitrate are dissolved in deionized water, the possible reactions that occur in the electrochemical cell are [4]: [[,5].

$$Ga(NO_3)_3 + H_2O \rightarrow Ga^{3+} + 3(NO_3)^-$$

$$NH_4NO_3 + H_2O \rightarrow NH_4{+}{+} (NO_3)^-$$

$$NH_4{+}{+} (NO_3)^- \rightarrow NH_3 + HNO_3$$

$$Ga\ (NO_3)_3 + NH_3 \rightarrow GaN + 3HNO_3$$

When a voltage is applied, the positive Ga^{3+} and NH_4^+ ions migrate to the cathode (Si or ITO substrate) in the presence of a high NH_4^+ concentration. Combination of these two ions forms the GaN thin film on the surface of the cathode.

2. Results and discussion

The XRD results of GaN thin films grown under the different conditions are shown in Fig. 2. The spectrum was dominated by peaks due to hexagonal GaN (JCPDS 50–0792). The small peak at 41° corresponds to cubic GaN (JCPDS 52–0791), which indicates that a small amount of cubic GaN might be present. Peaks due to the ITO substrate were also observed.

The structural parameters of the films were calculated from the XRD data and are shown in Table 2. These were compared to JCPDS files were appropriate and a close agreement was found. Also shown are the crystallite sizes (*t*) calculated using Scherrer's formula [13],

$$t = \frac{0.9\lambda}{B\cos\theta_B},$$

where λ is the wavelength of the incident X-rays (1.54056 Å for Cu $K_{\alpha 1}$), θ is Bragg angle and *B* is peak width at half maximum. Here it can be seen that the crystallites in the unstirred sample were significantly larger.

Fig. 3 shows the surface morphologies of representative samples of the various GaN thin films as observed by SEM. It can be seen that they are different and depend on both substrate and deposition conditions. The SEM images of the GaN thin films on ITO show that the films are porous, with unstirred films having a significant preferred orientation along with the (100) visible in Fig. 3c compared to the other films on ITO deposited with stirring. On Si (111) the film forms nanosheets of different sizes which uniformly cover the substrate surface.

2.1. Electrical characterization

The quality of the Ohmic contacts was investigated by splitting the Ohmic contact in two and performing an *I-V* measurement between the two halves of the contact. The *I-V* characteristics were symmetric and linear and corresponded to a resistance of 35 Ω see Fig. 4a. In Fig. 4 the *I-*

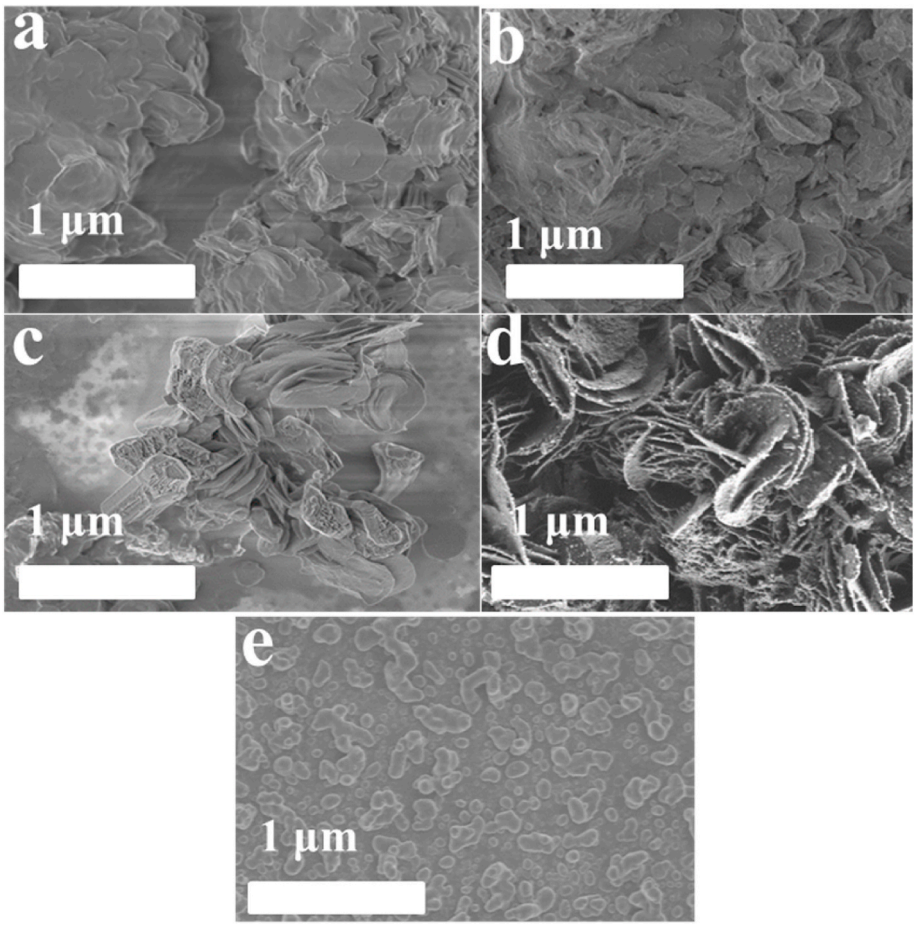

Fig. 3. SEM images of GaN thin films deposited under different conditions on ITO: (a) Sample *a* 1 mA/cm^2 for 3 h, (b) Sample *b* 1 mA/cm^2 for 12 h, (c) Sample *c* 0.7 mA/cm^2 for 3 h, (d) Sample *d* grown on Si(111) substrate 1 mA/cm^2 for 30 min and (e) Sample *e* grown on ITO 1 mA/cm^2 for 30 min.

V and *C-V* plots of Au/GaN/Al Schottky diodes are shown as measured at room temperature for Sample *d* (GaN on Si). The as-deposited sample showed rectifying behaviour of one order of magnitude. After irradiation by alpha-particles from an ^{241}Am source to a fluence of 6.13×10^{11} cm^{-2}, the rectification of the Schottky diodes increased by one order of magnitude and was accompanied by an increase in the series resistance across the diode. Using thermionic emission theory [14,15] and the plots in Fig. 4b, it was found that the ideality factor, n for the as-grown sample was 2.4, with a saturation current I_s of 1.2×10^{-6} A and a Schottky barrier height, ϕ_B of 0.58 eV. After irradiation, the aforementioned parameters changed to 2.6, 1.70×10^{-7} A and 0.64 eV, respectively as summarised in Table 3. Fitting the data from the *C-V* plots, it was found that the Schottky barrier height was 1.18 eV as-grown and this increased after irradiation to 2.20 eV, with the carrier concentration decreasing from 1.14×10^{18} cm^{-3} in the as-grown GaN to 1.10×10^{16} cm^{-3} after irradiation.

The difference between the *I-V* and *C-V* barrier heights can be understood by considering how variation in the barrier height across the surface of the diode would influence the measurement in each case. In the case of *I-V* characteristics, regions with different barrier heights are effectively in series, and the region with the best conduction (i.e. with the lowest barrier height) will dominate. Therefore, for Schottky diodes with barrier height variations, the *I-V* measurements are biased strongly to the lower barrier height and even a small area with a low barrier height may completely dominate the *I-V* characteristics. This effect is enhanced further by the exponential dependence of the current on the barrier height. In the case of *C-V* measurements, regions with different barrier heights have different capacitances, and the measured capacitance is the weighted average of these capacitances, so *C-V* measurements tend to average out differences in the barrier height. Consequently, barrier height inhomogeneities tend to reduce the *I-V* barrier height much more than the *C-V* barrier height. Another effect reducing the barrier height is image force lowering, which, due to the high carrier density of the material, would also play a role in this case [8].

2.2. DLTS results

Fig. 5 shows the DLTS spectrum obtained from as-deposited GaN in the range 50 K–300 K measured using the reverse bias voltage of −2 V, at a rate of window 80 s^{-1} and alpha-particle irradiated GaN in temperature range 40 K–350 K with a reverse bias of −1 V. Before alpha irradiation, there was one as-grown defect. Arrhenius plots shown in Fig. 6 were used to calculate activation energy and apparent capture cross-section of the defect observed. The activation of the energy of 0.32 eV in this study is similar to the activation energies of EO2, defect

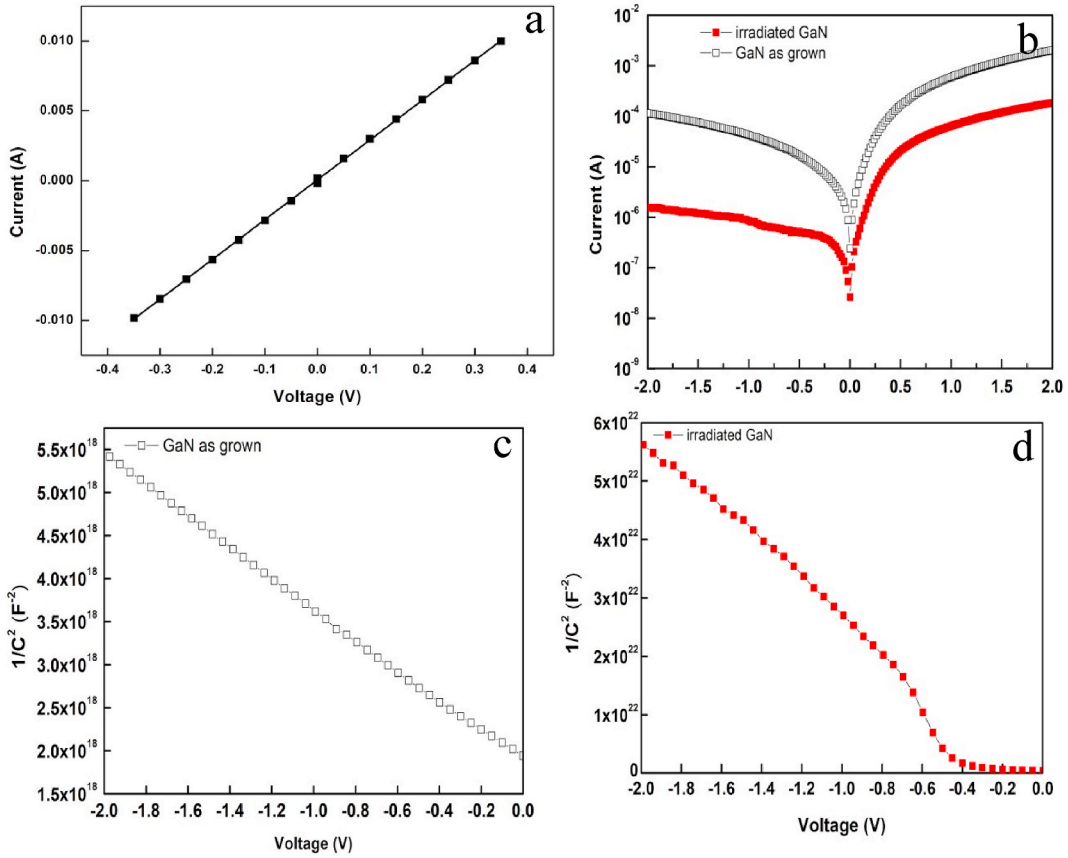

Fig. 4. (a) The IV graph for the Ohmic contact (b) Semilogarithmic *I-V* plot recorded before and after irradiation and (c), (d) the $1/C^2$ - *V* plots of the as-grown and irradiated Au/GaN/Al Schottky diode as measured at room temperature.

Table 3
The Schottky barrier height, ideality factor (*n*), saturation current (I_s) and *C-V* carrier concentration $N_D - N_A$ obtained from *I-V* and *C-V* measurements of Au/GaN/Al on Si.

Au/GaN/Si/Al	I_s (A)	φ_B (eV)		R_s (Ω)	*n*	$N_D - N_A$ (cm^{-3})
		I-V	C-V			
As grown	1.2×10^{-6}	0.58	1.18	550	2.4	1.1×10^{18}
After irradiation	1.2×10^{-7}	0.64	2.2[a]	7.5k	2.6	1.1×10^{16}

[a] Due to the nonlinear 1/C [2] vs V characteristics, the C-V barrier height is not accurate. The region −0.4 to 0 V was used for a linear fit.

investigated by Auret et al. [16] and the E2 by Tokuda [17] in as-grown epitaxial GaN. In these studies the activation energies were 0.27 eV, 0.23 eV and 0.32 eV, respectively. After alpha-particle irradiation of GaN, four defects were observed and the activation energies of the defects were 0.51 eV, 0.42 eV, 0.20 eV and 0.10 eV, labelled $E_{0.51}$, $E_{0.42}$, $E_{0.20}$ and $E_{0.10}$ respectively. In this study, the defects $E_{0.51}$ and $E_{0.20}$ were similar to the activation energies of EO5 and ER3 reported by Auret et al., after irradiation of epitaxial n-GaN by He^+ and protons [18]. The activation energy of those defects were 0.60 eV and 0.20 eV respectively. Also, the same activation energies for $E_{0.51}$ and $E_{0.20}$ were reported by Goodman et al. [19] after irradiation of MOVPE grown n-GaN by He-ion irradiation. Ngoepe et al. [20] also observed the same defects after irradiating n-GaN with Xe-ions. The defect $E_{0.10}$ had a similar activation energy to G_1, ED1 and ER1 which were reported by Umana-Membreno et al. [21], Polenta et al. [22] and Auret et al. [18] respectively, however, the $E_{0.10}$ has a capture cross section five orders of magnitude larger, and is therefore believed to be a different defect, not previously observed. The $E_{0.20}$ defect in this study is similar to the D_1

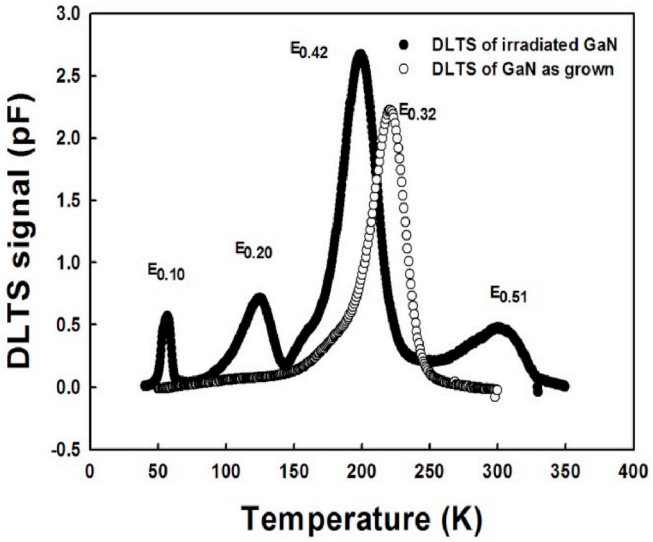

Fig. 5. DLTS spectra of as-deposited and α-irradiated GaN on Si deposited by electrochemical deposition.

observed by Fang et al. which might be related to a nitrogen or gallium vacancy [23]. While traps $E_{0.51}$, $E_{0.42}$ and $E_{0.32}$ would possibly be assigned to the N_{Ga} related defect [23,24].

The activation energy and apparent capture cross-section (σ_a) of each defect observed in this study compared to previous work are shown in Table 4. The capture cross-section of the activation energies in the

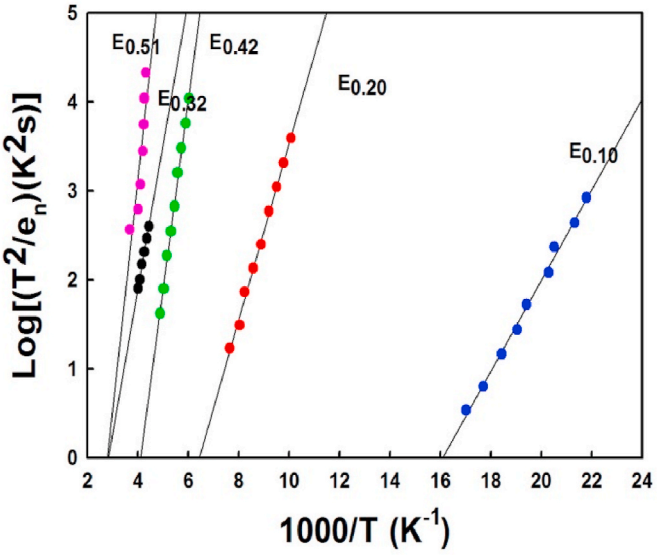

Fig. 6. The Arrhenius plot of defects in as-grown and α-irradiated Au/GaN/Al devices.

Table 4
Electronic properties of the defects detected by DLTS in the as-grown and α-irradiated GaN thin films.

Process	Defect label current work	Defect level (eV)	σ_a (cm^2) current work	Similar defect activation energy (eV)	Similar capture cross section (cm^2)	Reference
As deposited	$E_{0.32}$	0.32	1.9×10^{-17}	0.27	8×10^{-15}	[16]
				0.31	3.6×10^{-16}	[17]
α-irradiation	$E_{0.10}$	0.10	1.8×10^{-13}	–	–	–
α-irradiation	$E_{0.20}$	0.20	1.5×10^{-15}	0.22	3.8×10^{-16}	[10]
				0.20	$\sim 4 \times 10^{-16}$	[16][18]
				0.20	8.4×10^{-16}	[19]
						[23]
α-irradiation	$E_{0.42}$	0.42	3.5×10^{-13}	0.45	1.3×10^{-13}	[10]
				0.40	1.4×10^{-15}	[17]
α-irradiation	$E_{0.51}$	0.51	1.2×10^{-14}	0.61	1×10^{-14}	[16]
				0.57	1.1×10^{-15}	[17]
				0.48	1.5×10^{-15}	[20]

current work were found differ from the previous literature in some cases, but this can be attributed to different of the growth technique used in this study.

3. Conclusion

GaN thin films were successfully synthesized by electrochemical deposition on both Si and ITO substrates. XRD analysis showed that the hexagonal wurtzite structure dominated with a small amount of cubic phase of the GaN present and this was supported by SEM studies of the morphology of the GaN thin films. The *I-V* and *C-V* measurements before and after irradiation were determined, and the Schottky barrier height and ideality factor the Au/GaN/Al Schottky diode on as-grown GaN and after irradiation were obtained from *I-V* measurements to be 0.58 eV, 2.4 and 0.64 eV and 2.6 respectively as seen in Table 3. DLTS measurements on the as-grown GaN thin film showed a defect with activation energy 0.32 eV. This defect corresponds well to previously reported defects in bulk GaN grown by different growth techniques. After irradiating GaN with alpha-particles four defect peaks were observed, namely, $E_{0.51}$, $E_{0.42}$, $E_{0.20}$, and $E_{0.10}$ and defects with similar activation energies have previously been reported in single-crystal materials. This study has revealed that electrochemical deposition is a more cost-effective and simple process of synthesising GaN compared to the more expensive techniques such as metal-organic chemical vapor deposition [1,25,26], molecular beam epitaxy [2], hydride vapor-phase epitaxy (HVPE) [3,27] in terms of the electrical characteristics of the films and the properties of Schottky diodes.

CRediT authorship contribution statement

Abdulraoof I.A. Ali: Conceptualization, Methodology, Investigation, Writing - original draft. **Helga T. Danga:** Investigation, Writing - original draft. **Jacqueline M. Nel:** Conceptualization, Methodology, Writing - review & editing, Supervision, Project administration, and, Funding acquisition. **Walter E. Meyer:** Supervision, Writing - review & editing.

Declaration of competing interest

The authors declare that they have no known competing financial interests or personal relationships that could have appeared to influence the work reported in this paper.

Acknowledgement

The authors would like to thank the South African National Research Foundation (NRF) for financial support during this study under Grant number 111744.

References

[1] T. Kuykendall, P. Pauzauskie, S. Lee, Y. Zhang, J. Goldberger, P. Yang, Metalorganic chemical vapor deposition route to GaN nanowires with triangular cross sections, Nano Lett. 3 (8) (2003) 1063–1066.

[2] Y. Huang, X. Duan, Y. Cui, C.M. Lieber, Gallium nitride nanowire nanodevices, Nano Lett. 2 (2) (2002) 101–104.

[3] Z.Q. Fang, D.C. Look, W. Kim, Z. Fan, A. Botch karev, and H. Morkoç, Appl. Phys. Lett. 72 (1998) 2277.

[4] P.R. Hageman, V. Kirilyuk, W.H.M. Corbeek, J.L. Weyher, B. Lucznik, M. Bockowski, S. Müller, Thick GaN layers grown by hydride vapor-phase epitaxy: hetero-versus homo-epitaxy, J. Cryst. Growth 255 (3–4) (2003) 241–249.

[5] R.K. Roy, A.K. Pal, Synthesis of gallium nitride films by a novel electrodeposition route, Mater. Lett. 59 (17) (2005) 2204–2209.

[6] K. Al-Heuseen, M.R. Hashim, One-step synthesis of GaN thin films on Si substrate by a convenient electrochemical technique at low temperature for different durations, J. Cryst. Growth 324 (1) (2011) 274–277.

[7] K.H. Ploog, O. Brandt, H. Yang, A. Trampert, MBE growth and characteristics of cubic GaN, Thin Solid Films 306 (2) (1997) 231–236.

[8] D.K. Schroder, Semiconductor Material and Device Characterization, John Wiley & Sons, 2015.

[9] F.D. Auret, S.A. Goodman, G. Myburg, S.E. Mohney, J.M. De Lucca, Processing-induced electron traps in n-type GaN, Mater. Sci. Eng., B 82 (1–3) (2001) 102–104.

[10] P.J. Van Rensburg, F.D. Auret, V.S. Matias, A. Vantomme, Electrical characterization of rare-earth implanted GaN, Phys. B Condens. Matter 404 (22) (2009) 4411–4414.

[11] M. Mamor, F.D. Auret, S.A. Goodman, W.E. Meyer, G. Myburg, Electronic and transformation properties of a metastable defect introduced in epitaxially grown boron-doped p-type Si by alpha particle irradiation, Appl. Phys. Lett. 72 (24) (1998) 3178–3180.

[12] D.V. Lang, Deep-level transient spectroscopy: a new method to characterize traps in semiconductors, J. Appl. Phys. 45 (7) (1974) 3023–3032.

[13] A.L. Patterson, The Scherrer formula for X-ray particle size determination, Phys. Rev. 56 (10) (1939) 978.

[14] E.H. Rhoderick, Metal-semiconductor contacts, IEE Proc. I-Solid-State and Electron Devices 129 (1) (1982) 1.

[15] S.M. Sze, K.K. Ng, Physics of Semiconductor Devices, John wiley & sons, 2006.

[16] F.D. Auret, S.A. Goodman, F.K. Koschnick, J.M. Spaeth, B. Beaumont, P. Gibart, Electrical characterization of two deep electron traps introduced in epitaxially grown n-GaN during He-ion irradiation, Appl. Phys. Lett. 73 (25) (1998) 3745–3747.

[17] Y. Tokuda, Traps in MOCVD n-GaN studied by deep level transient spectroscopy and minority carrier transient spectroscopy, in: CS MANTECH Conference, 2014, May, pp. 19–24.

[18] F.D. Auret, S.A. Goodman, F.K. Koschnick, J.M. Spaeth, B. Beaumont, P. Gibart, Proton bombardment-induced electron traps in epitaxially grown n-GaN, Appl. Phys. Lett. 74 (3) (1999) 407–409.

[19] S.A. Goodman, F.D. Auret, F.K. Koschnick, J.M. Spaeth, B. Beaumont, P. Gibart, Radiation induced defects in MOVPE grown n-GaN, Mater. Sci. Eng., B 71 (1–3) (2000) 100–103.

[20] P.N.M. Ngoepe, W.E. Meyer, F.D. Auret, E. Omotoso, T.T. Hlatshwayo, V. A. Skuratov, M. Diale, Deep level transient spectroscopy characterisation of Xe irradiated GaN, Nucl. Instrum. Methods Phys. Res. Sect. B Beam Interact. Mater. Atoms 409 (2017) 69–71.

[21] G.A. Umana-Membreno, J.M. Dell, T.P. Hessler, B.D. Nener, G. Parish, L. Faraone, U.K. Mishra, 60 Co gamma-irradiation-induced defects in n-GaN, Appl. Phys. Lett. 80 (23) (2002) 4354–4356.

[22] L. Polenta, Z.Q. Fang, D.C. Look, On the main irradiation-induced defect in GaN, Appl. Phys. Lett. 76 (15) (2000) 2086–2088.

[23] Z.Q. Fang, D.C. Look, W. Kim, Z. Fan, A. Botchkarev, H. Morkoç, Deep centers in n-GaN grown by reactive molecular beam epitaxy, Appl. Phys. Lett. 72 (18) (1998) 2277–2279.

[24] H.K. Cho, C.S. Kim, C.H. Hong, Electron capture behaviors of deep level traps in unintentionally doped and intentionally doped n-type GaN, J. Appl. Phys. 94 (3) (2003) 1485–1489.

[25] X.M. Shen, D.G. Zhao, Z.S. Liu, Z.F. Hu, H. Yang, J.W. Liang, Space-charge-limited currents in GaN Schottky diodes, Solid State Electron. 49 (5) (2005) 847–852.

[26] C. Lu, S.N. Mohammad, Validity/invalidity of Schottky-Mott rules for Schottky contacts to III-V nitride semiconductor heterostructures, Appl. Phys. Lett. 89 (16) (2006), 162111.

[27] Y. Zhou, D. Wang, C. Ahyi, C.C. Tin, J. Williams, M. Park, E.A. Preble, Temperature-dependent electrical characteristics of bulk GaN Schottky rectifier, J. Appl. Phys. 101 (2) (2007), 024506.